Rigorous analysis of diffraction gratings of arbitrary profiles using virtual photonic crystals

Wei Jiang and Ray T. Chen

Microelectronics Research Center and Department of Electrical and Computer Engineering, The University of Texas at Austin, Austin, Texas 78758

Received February 10, 2006; revised April 4, 2006; accepted April 4, 2006; posted April 7, 2006 (Doc. ID 67976)

A new approach is developed to calculate diffraction efficiency for a dielectric grating with an arbitrary refractive index profile. By treating a one-dimensional grating as a segment of a virtual two-dimensional (2D) photonic crystal, we exploit a rigorous theory of photonic crystal refraction and calculate the diffraction efficiencies. We expand, analytically in many cases, the dielectric function of the grating into 2D Fourier series. We find the eigenmodes for the virtual photonic crystal, and then use these eigenmodes to match the boundary conditions by solving a set of linear equations. In two such simple steps, the diffraction efficiencies can be computed rigorously without slicing the grating into thin layers.

OCIS codes: 050.1950, 050.1960.

1. INTRODUCTION

Dielectric gratings have been subject to extensive studies in the past due to their wide applications in holography, spectroscopy, lasers, and optoelectronics.[1–10] Numerous devices and systems have been conceived and built with dielectric gratings as essential functional parts. Among them, distributed-feedback lasers, optical spectrum analyzers, and wavelength division demultiplexers are well-known examples. In many applications, one of the most essential performance characteristics of gratings is diffraction efficiency, which has been analyzed by numerous theoretical techniques. During the past two decades, layering approaches[2–6] have gained popularity in numerical modeling of dielectric gratings with arbitrary profiles. Generally, these approaches slice a surface-relief grating into a large number of thin layers, each of which can be considered uniform in the thickness direction. The electromagnetic fields on the front and back surfaces of each layer can be easily related by solving Maxwell's equations. The relation between the fields on the front and back surfaces is commonly expressed in certain matrix form, often called transfer matrices or T matrices.[6] Once the T matrices are calculated for each layer, one can, in principle, multiply the T matrices sequentially to obtain the overall transfer matrix that relates the front and back surfaces of the entire grating. Because it turned out that such multiplication resulted in numerical instability for a large number of layers, a number of alternative formulations,[3–6] including the R-matrix or S-matrix approaches as reviewed in Ref. 6, were later devised to overcome the instability issue. These advancements have greatly improved the accuracy and efficiency of calculating the diffraction efficiencies for dielectric gratings with arbitrary profiles. In this paper, we present a new approach to calculating diffraction efficiency by treating an arbitrary grating as one layer of a photonic crystal, which retains the structural signature of the original grating. This rigorous approach is mathematically simple and allows us to exploit the analytic Fourier expansion of many common grating profiles.

2. VIRTUAL PHOTONIC CRYSTAL

In recent years, photonic crystal research has further broadened our view of dielectric gratings by introducing the concept of photonic bands and bandgaps. The study of light refraction on a photonic crystal surface, or the superprism effect,[11] prompted us to reconsider certain issues that have not received much attention in grating diffraction. These include the characteristics of light refraction on a single photonic crystal surface, which sometimes exhibits abnormality or high sensitivity to wavelengths and incident angles.[11] The high sensitivity mandates numerical accuracy beyond popular computation techniques such as the finite-difference time-domain method. Recently, we developed a rigorous theoretic framework to model the refraction, transmission, and propagation inside a dielectric photonic crystal that has an arbitrary lattice type and arbitrary surface orientation.[12] Our theory does not need to discretize a photonic crystal or slice it into many thin layers. Motivated by that work, we have developed a rigorous theory of modeling grating diffraction without slicing a grating into thin layers. As discussed in our previous work,[12] our approach is applicable to both TE and TM polarizations, although for simplicity we will focus on one polarization here.

The key idea of this work is to consider a grating with one-dimensional periodicity as part of a two-dimensional (2D) photonic crystal. In Fig. 1 we illustrate this concept. For the grating shown in Fig. 1(a), the corresponding virtual 2D photonic crystal is shown in Fig. 1(b). A unit cell of the photonic crystal is indicated by the dotted lines in Fig. 1(b). The grating can be seen as a segment of the 2D photonic crystal, having only one period along the y axis. In fact, covering regions I and III and looking at region II

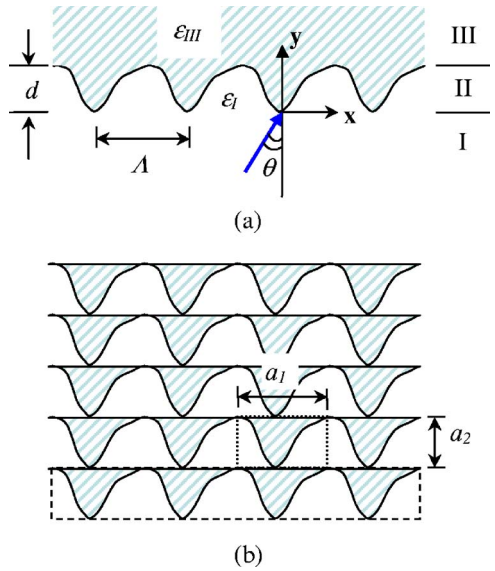

Fig. 1. (Color online) Concept of a virtual photonic crystal, where we treat a grating as a single layer of a 2D photonic crystal. (a) A surface-relief grating with an arbitrary profile. The origin of the coordinate system is located on the farthest extrusion of the surface. Three regions are marked by I, II, and III. (b) The corresponding virtual 2D photonic crystal, where a unit cell is indicated by dotted lines. For a rectangular lattice $a_1=\Lambda$, $a_2=d$. The layer actually present in the grating problem is enclosed by dashed lines.

only in Fig. 1(a), one could not tell whether the dielectric structure between $y=0$ and $y=d$ is a grating or is a part of a photonic crystal. Either view of the structure in region II is valid. Therefore, we can convert the grating diffraction problem into a transmission/reflection problem for a monolayer of photonic crystal. Note that except for one monolayer enclosed by the dashed lines in Fig. 1(b), the other part of the 2D photonic crystal does not physically exist. For this reason, we call it a virtual photonic crystal.

In principle, the unit cell could be an arbitrary parallelogram with its base parallel to the grating surface (or x axis in the diagram). For simplicity, we choose a rectangular unit cell throughout this work. The 2D Fourier coefficients of the space-dependent dielectric function $\varepsilon(\mathbf{x})$ of such a photonic crystal can then be calculated as

$$\varepsilon(\mathbf{G}) = \frac{1}{A}\int\int \mathrm{d}x\mathrm{d}y\, \exp(-i\mathbf{G}\mathbf{x})\epsilon(\mathbf{x}), \tag{1}$$

where A is the area of a unit cell. The spatially varying dielectric constant is given by $\varepsilon(\mathbf{x})=\Sigma_{\mathbf{G}}\varepsilon(\mathbf{G})\exp(i\mathbf{G}\cdot\mathbf{x})$, where $\mathbf{G}$ is a reciprocal lattice vector, and

$$\mathbf{G}_{l,m} = l\mathbf{b}_1 + m\mathbf{b}_2.$$

Here $\mathbf{b}_1$ and $\mathbf{b}_2$ are the basis vectors of the reciprocal lattice of the virtual photonic crystal. For a finite Fourier series, we assume $-L\leqslant l\leqslant L$, $-M\leqslant m\leqslant M$, and the total number of Fourier components is $N=(2L+1)(2M+1)$.

From the Fourier analysis viewpoint, slicing a grating into thin layers means that the Fourier coefficients of the grating are essentially calculated by the staircase approximation of Fourier integrals along the y direction. Such approximated Fourier coefficients converge relatively slowly with the number of layers. There are other schemes that can approximate the Fourier integral of Eq. (1) with faster convergence, but they generally resort to techniques beyond the staircase approximation that is characteristic of the layering approaches. Furthermore, to achieve stability, the transfer-matrix approach requires relatively complicated matrix operations such as matrix inversion for iteration through each layer.[6] The overall transfer matrix of the entire grating depends on the original transfer matrix of each layer in a complicated way, which makes evaluation of the error bound of the overall calculation a difficult task. The method to be presented here shows a promising way to avoid these issues. It separates the calculation of the 2D Fourier coefficients from the electromagnetic field calculation; therefore the 2D Fourier coefficients can be evaluated with faster and more accurate numerical algorithms. For many regularly shaped surface-relief gratings, it is often possible to analytically calculate the Fourier coefficients.

3. THEORY FOR DIFFRACTION EFFICIENCY

Consider the TE polarization (called TM in photonic crystal research), for which the magnetic field lies in plane. Generally, Maxwell's equations can be converted into a second-order partial differential equation, which has a handy form for the 2D TE polarization:

$$\nabla^2 E(\mathbf{x}) + \omega^2\varepsilon(\mathbf{x})E(\mathbf{x}) = 0, \tag{2}$$

where ω is the circular frequency (assume the speed of light $c=1$), and

$$E(\mathbf{x}) = \exp(i\mathbf{k}\cdot\mathbf{x})\sum_{\mathbf{G}} E(\mathbf{G})\exp(i\mathbf{G}\cdot\mathbf{x}), \tag{3}$$

according to the Bloch theorem. Equation (1) can be written as

$$-[(k_x+G_x)^2 + (k_y+G_y)^2]E(\mathbf{G}) + \omega^2\sum_{\mathbf{G}'}\varepsilon(\mathbf{G}-\mathbf{G}')E(\mathbf{G}') = 0. \tag{4}$$

For the grating diffraction problem, we know the wavelength λ and the incident angle, from which the circular frequency ω and tangential incident wave k_x can be easily obtained. With ω and k_x known, we need to solve Eq. (4) to find the eigenvalues $k_y(s)$, $s=1,2,\ldots,2N$, and the corresponding eigenvectors $E_s(\mathbf{G})$. The eigenvalue problem can be reformulated into a matrix form:

$$(k_y^2[I] + 2k_y[B] + [C])[E] = 0, \tag{5}$$

where $[I]$, $[B]$, and $[C]$ are N-by-N matrices, particularly $[I]$ is the identity matrix; and $[E]$ is a N-by-1 column vector. Such an eigenvalue problem can be easily converted into an ordinary eigenvalue problem by assigning $[Z]=(k_y[I]+[B])[E]$. The eigenvalue problem now takes the expanded form

$$\begin{bmatrix} -B & I \\ D & -B \end{bmatrix}\begin{bmatrix} E \\ Z \end{bmatrix} = k_y\begin{pmatrix} E \\ Z \end{pmatrix}, \tag{6}$$

where $[D]=[B]^2-[C]$. It is straightforward to show that $[B]$ is a diagonal matrix in this problem; therefore the calculation of $[B]^2$ is straightforward. Note that one may as-

sign a different $[Z]$, for example, $[Z]=k_y[E]$, and obtain a different form of an expanded eigenvalue problem; nevertheless the eigenvalues k_y and the corresponding eigenvectors E remain the same. Note that if $[I]$ is replaced by an arbitrary matrix $[A]$, then an expanded $2N$-by-$2N$ eigenvalue problem similar to Eq. (6) can still be obtained through a standard approach.[13] However, one may again define $[Z]$ in convenient ways without following the standard approach. We choose the current form of Eq. (6) primarily for mathematical simplicity. For the current problem, one can show that

$$B_{\mu\nu} = \delta_{\mu\nu}(\mathbf{G}_\mu)_y,$$

$$C_{\mu\nu} = \delta_{\mu\nu}\{(\mathbf{G}_\mu)_y^2 + [k_x + (\mathbf{G}_\mu)_x]^2\} - \omega^2\varepsilon(\mathbf{G}_{\mu\nu}),$$

$$D_{\mu\nu} = \omega^2\varepsilon(\mathbf{G}_{\mu\nu}) - [k_x + (\mathbf{G}_\mu)_x]^2\delta_{\mu\nu},$$

where $\mu, \nu = 1, 2, \ldots, N$ are linear indices for (l,m) pairs. That is, for each pair (l,m) where $l=-L, -L+1, \ldots L-1, L$, and $m=-M, -M+1, \ldots, M-1, M$, a unique number μ (or ν) between 1 and N is assigned to it. Moreover, we define $\mathbf{G}_{\mu\nu} \equiv \mathbf{G}_\mu - \mathbf{G}_\nu$.

Apparently, there are $2N$ eigenvalues. Typically, N is around 600–1000. However, as proved in Ref. 12, the eigenvalues are highly degenerate. Only the $2(2L+1)$ eigenvalues in the first Brillouin zone (BZ), defined by

$$-b_2/2 \leqslant \mathrm{Re}\, k_y < b_2/2, \tag{7}$$

should be considered. As discussed in Ref. 12, those eigenvalues outside the first BZ differ from those inside by $m\mathbf{b}_2$, where $m=-M, -(M+1), \ldots, M$. Yet the real-space eigenfunctions $E(\mathbf{x})$ for those eigenvalues outside are identical to those in the first BZ. This reveals that the former are plainly the replicas of the latter with the apparent difference of k_y attributed to the periodic BZ scheme.[12]

This degeneracy ensures that we only need to calculate a small subset of eigenvalues $k_y(s)$ satisfying inequality (7), which contributes the numerical efficiency of this approach for a large value of M. Those eigenmodes outside the first BZ have no use in the subsequent calculations just like those replica eigenmodes have no use in the photonic crystal refraction calculations.[12] Furthermore, for sufficiently large L, M (e.g., $L, M > 4$ in most cases), we observed that the majority of the $2(2L+1)$ eigenvalues in the first BZ could be approximated by

$$k_y \approx \pm i\sqrt{[k_x + (\mathbf{G}_{l0})_x]^2 - \varepsilon(0)\omega^2},$$

$$l = \pm L_0, \pm (L_0+1), \ldots, \pm L, \tag{8}$$

where typically $L_0 > 2$. To prove this, consider an eigenvector whose largest component is $E(\mathbf{G}_{lm})$, where $|\mathbf{G}_{lm}|$ is large enough. Note that for a sufficiently large $\mathbf{G}_{lm}$, the first part of Eq. (4), which is proportional to $(\mathbf{k}+\mathbf{G})^2$, dominates over the second part that contains $\epsilon(\mathbf{G}-\mathbf{G}')$. Keeping only the leading term of the sum in Eq. (4) and restricting k_y to the first BZ, one readily obtains approximation (8). It is straightforward to derive the corresponding approximated eigenvectors. With such good approximated eigenvalues (usually less than 2% error) as a starting point, one can numerically find the accurate value of each corresponding eigenvalue very fast. For a large value of L, all but a few eigenvalues can be obtained through this highly expedited technique. It is not absolutely necessary to use this technique for the grating calculations presented here that involve only 2D photonic crystals. We developed this technique primarily for simulating the superprism effect in a three-dimensional photonic crystal, where the computational workload is more demanding. The details of three-dimensional photonic crystal computation will be presented elsewhere.

Unlike for a semi-infinite photonic crystal, in principle, there is no need to separate the up and down modes[12] for a grating, which essentially is a photonic crystal with a finite dimension along the y axis. Neither up modes nor down modes diverge under such circumstances and both are physically present. Nevertheless, for numerical stability, certain partition of the evanescent modes is helpful as we shall see.

With eigenmodes of the virtual photonic crystal, the boundary conditions can now be solved through a set of linear equations. Consider the grating shown in Fig. 1(a). The incident medium, the grating, and the half-space behind the grating are called region I, II, and III, respectively. A planar wave with unity amplitude impinges upon the grating surface at an angle θ. First, we write down the electric field in three regions:

$$E_{\mathrm{I}}(\mathbf{x}) = \exp(i\mathbf{q}_0\mathbf{x}) + \sum_l r_l \exp(i\mathbf{p}_l\mathbf{x}),$$

$$E_{\mathrm{II}}(\mathbf{x}) = \sum_s \sum_{l,m} c_s E_s(\mathbf{G}_{lm}) \exp[i(k_x + lb_1)x + i(k_y(s) + mb_2)y],$$

$$E_{\mathrm{III}}(\mathbf{x}) = \sum_l t_l \exp(i\mathbf{v}_l\mathbf{x}), \tag{9}$$

where

$$\mathbf{p}_l = (q_{0x} + lb_1)\mathbf{e}_x - \sqrt{\varepsilon_{\mathrm{I}}\omega^2 - (q_{0x} + lb_1)^2}\,\mathbf{e}_y,$$

$$\mathbf{v}_l = (q_{0x} + lb_1)\mathbf{e}_x + \sqrt{\varepsilon_{\mathrm{III}}\omega^2 - (q_{0x} + lb_1)^2}\,\mathbf{e}_y;$$

and c_s, r_l, and t_l represent the complex amplitudes of the eigenmode $E_s(\mathbf{x})$, reflected wave, and transmitted wave, respectively. Note that $q_{0x} \equiv k_x$. Again, we emphasize that only $2(2L+1)$ eigenmodes $E_s(\mathbf{G})$ whose eigenvalues $k_y(s)$ are in the first BZ are included in Eqs. (9).

By combining the boundary conditions for entering and exiting a photonic crystal, one can now derive the complete boundary conditions at the front and back surfaces of the grating:

$$\delta_{l,0} + r_l = \sum_s c_s \sum_m E_s(\mathbf{G}_{lm}),$$

$$q_{0y}\delta_{l,0} + p_{l,y}r_l = \sum_s c_s \sum_m [k_y(s) + mb_2]E_s(\mathbf{G}_{lm}),$$

$$\exp(iv_{l,y}d)t_l = \sum_s c_s \exp[ik_y(s)d] \sum_m E_s(\mathbf{G}_{lm}),$$

$$v_{l,y}\exp(iv_{l,y}d)t_l = \sum_s c_s \exp[ik_y(s)d] \times \sum_m [k_y(s)+mb_2]E_s(\mathbf{G}_{lm}). \quad (10)$$

The first two equations are for the front surface and the last two are for the back surface. The first and third equations are based on the continuity of the electric field, and the second and fourth are based on the continuity of the tangential component of the magnetic field. Note that if we had not chosen a rectangular unit cell (i.e., a_2 is not parallel to the y axis, but a_1 must always be parallel to the grating surface or the x axis), $\mathbf{b}_1$ may not be parallel to the x axis. Then it can be easily shown that the term mb_2 in Eqs. (9) and (10) would become $lb_{1y}+mb_2$. There should be a factor $\exp[i(lb_{1y}+mb_2)d]$ for each term on the right-hand side of the last two equations of Eqs. (10). However, for a rectangular cell, it is straightforward to show that $\exp[i(lb_{1y}+mb_2)d]=1$ because $b_2=2\pi/d$ for a grating and $b_{1y}=0$ by choosing a rectangular cell.

Because complex $k_y(s)$ eigenvalues appear in conjugate pairs, the coefficients containing $\exp[ik_y(s)d]$ for $\mathrm{Im}\,k_y(s)<0$ for a large d may dominate over other terms in Eqs. (10).[14] To avoid this problem, we define

$$\tilde{c}_s = \begin{cases} c_s \exp[ik_y(s)d] & \mathrm{Im}\,k_y(s)<0 \\ c_s & \text{otherwise} \end{cases}. \quad (11)$$

Also, we define $\tilde{t}_l = t_l \exp(i\nu_{l,y}d)$. Now Eqs. (10) become

$$\begin{aligned}
\delta_{l,0}+r_l &= \sum_{s+}\tilde{c}_{s+}\sum_m E_{s+}(\mathbf{G}_{lm}) + \sum_{s-}\tilde{c}_{s-} \times \exp[-ik_y(s^-)d]\sum_m E_{s-}(\mathbf{G}_{lm}), \\
q_{0y}\delta_{l,0}+p_{l,y}r_l &= \sum_{s+}\tilde{c}_{s+}\sum_m [k_y(s^+)+mb_2]E_{s+}(\mathbf{G}_{lm}) + \sum_{s-}\tilde{c}_{s-}\exp[-ik_y(s^-)d] \times \sum_m [k_y(s^-)+mb_2]E_{s-}(\mathbf{G}_{lm}), \\
\tilde{t}_l &= \sum_{s+}\tilde{c}_{s+}\exp[ik_y(s^+)d]\sum_m E_{s+}(\mathbf{G}_{lm}) + \sum_{s-}\tilde{c}_{s-}\sum_m E_{s-}(\mathbf{G}_{lm}), \\
v_{l,y}\tilde{t}_l &= \sum_{s+}\tilde{c}_{s+}\exp[ik_y(s^+)d]\sum_m [k_y(s^+) + mb_2]E_{s+}(\mathbf{G}_{lm}) + \sum_{s-}\tilde{c}_{s-}\sum_m [k_y(s^-) + mb_2]E_{s-}(\mathbf{G}_{lm}), \quad (12)
\end{aligned}$$

where $s-$ refers to those modes with $\mathrm{Im}\,k_y(s)<0$, whereas $s+$ refers to other modes. This new form ensures the numerical stability when solving the linear equations.

For each diffraction order with real $\mathbf{p}_l$, $\mathbf{v}_l$, the diffraction efficiency is given by normalized y components of Poynting vectors that measure the power-splitting ratios

$$\text{reflection:} \quad \frac{|r_l|^2|p_{l,y}|}{q_{0y}},$$

$$\text{transmission:} \quad \frac{|t_l|^2 v_{l,y}}{q_{0y}}.$$

As mentioned above, for common grating profiles, the Fourier components $\epsilon(\mathbf{G})$ can be calculated analytically. In fact, the Fourier components for a sinusoidal profile are found to have the form

$$\epsilon(\mathbf{G}_{lm}) = \begin{cases} \frac{1}{2}(\epsilon_{\mathrm{I}}+\epsilon_{\mathrm{III}})\delta_{l,0} + \frac{1}{4}(\epsilon_{\mathrm{III}}-\epsilon_{\mathrm{I}})(\delta_{l,1}+\delta_{l,-1}) & m=0 \\ \frac{\epsilon_{\mathrm{III}}-\epsilon_{\mathrm{I}}}{2\pi m}[i\delta_{l,0}+(-1)^m i^{l-1}J_l(m\pi)] & m\neq 0 \end{cases}, \quad (13)$$

where $J_l(x)$ is the lth-order Bessel function of the first kind. The diffraction efficiencies for a sinusoidal grating are shown in Fig. 2 for varying groove depths. The crosses represent the published results from Fig. 4 of Ref. 2 (data obtained by computer software from the scanned image of the original plot). Our results are in excellent agreement with those of Ref. 2.

The Fourier components of a sawtooth profile are found to have the form

$$\epsilon(\mathbf{G}_{lm}) = \begin{cases} \frac{1}{2}(\epsilon_{\mathrm{I}}+\epsilon_{\mathrm{III}}) & l=m=0 \\ (\epsilon_{\mathrm{III}}-\epsilon_{\mathrm{I}})/(2\pi i l) & l\neq 0, \quad m=0 \\ -\frac{(\epsilon_{\mathrm{III}}-\epsilon_{\mathrm{I}})}{2\pi i m}[\delta_{l,0}-\delta_{l+m,0}] & m\neq 0 \end{cases}. \quad (14)$$

The diffraction efficiencies for a sawtooth grating are shown in Fig. 3. Again, we compare our results with those obtained by reading the scanned plot of Fig. 7 in Ref. 2, and the agreement is excellent.

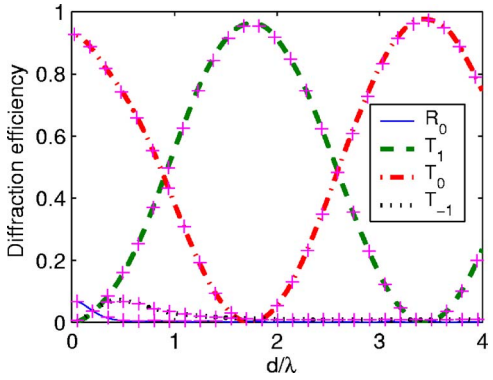

Fig. 2. (Color online) Diffraction efficiencies for a sinusoidal grating, where $\epsilon_{\mathrm{I}}=1$, $\epsilon_{\mathrm{III}}=2.5$, $\lambda=\Lambda$, and $\theta=30°$. One reflection order R_0 and three transmission orders T_{-1}, T_0, T_1 are shown. The crosses represent the published results from Fig. 4 of Ref. 2. Our results are in excellent agreement with those of Ref. 2.

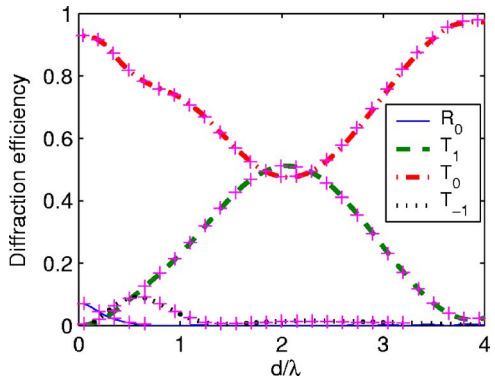

Fig. 3. (Color online) Diffraction efficiencies for a sawtooth grating, where $\epsilon_{\mathrm{I}}=1$, $\epsilon_{\mathrm{III}}=2.5$, $\lambda=\Lambda$, and $\theta=30°$. One reflection order and three transmission orders are shown. The crosses represent the data from Fig. 7 of Ref. 2. The agreement is excellent.

4. DISCUSSION

Generally, the R-or S-matrix approaches require a series of complicated matrix operations. Our method requires only two matrix operations: solving eigenvalues and then solving a linear equation. In this way, as long as we have a good eigenvalue solver and a good linear equation solver, there is no need for specialized, complicated algorithms for numerical stability. As such, researchers could focus more on the optics than on computational details. Note that good eigenvalue solvers and linear equation solvers are available from open sources such as ARPACK and LAPACK. Our approach separates the calculation of Fourier coefficients of the grating from the diffraction efficiency calculation. Therefore, the accuracy of the Fourier integral in Eq. (1) does not depend on the method we used to calculate the diffraction efficiencies. In the layering approaches, the number of layers required for the calculation of the diffraction efficiency essentially determines the accuracy of the implicit Fourier integral. Furthermore, the evaluation of error bounds for our method would be much simpler than for the conventional layering approaches because our method has only two steps. In contrast, it is highly complicated and therefore impractical to evaluate the overall error bound of the R-and S-matrix approaches that involve a long series of repeated matrix operations, including matrix multiplication and inversion. Developing a detailed procedure of rigorously estimating the error bound for this method could be closely related to the perturbation techniques to be discussed below, resulting in an interesting direction for further study.

We would like to point out one interesting correspondence between our method and the layering approach. In our method, one seeks the eigenvalue k_y of a matrix $[V]$, whereas the layering involves a matrix $\exp(i[V]d)$ that connects the electromagnetic fields on the front and back surfaces. If the original eigenvalues of $[V]$ have comparable magnitudes, the eigenvalues of $\exp(i[V]d)$ would generally distribute over a much larger numerical range as most eigenvalues of $[V]$ are complex.

Furthermore, it could be conductive to incorporate our method into the R- or S-matrix approach. With our method, one can now divide a deep grating into a small number (e.g., three or four) of relatively thick layers. Then one may use the R- or S-matrix approach recursively through these few layers to obtain the overall matrix for the entire grating. The transmission through each thick layer is rigorously computed with our new method. This differs from the conventional layering method in that each layer does not have to be very thin (this was required for the staircase approximation in the conventional method). This certainly offers flexibility and advantages unavailable prior to this work. For extremely deep gratings, such a method of combining the current method with an R-matrix or S-matrix approach may be especially useful. It would be an interesting problem to study how to choose the maximum layer thickness or the minimum number of layers to optimize the numerical efficiency against the accuracy for an extremely deep grating.

Meanwhile, follow-up work could help to evaluate whether perturbation techniques can become more effective using this theory as a starting point. In some cases, with the analytic formulas of $\varepsilon(\mathbf{G})$, it might be possible to analytically carry out the problem solution to a deeper level with common matrix perturbation theories[15] or, in a form more familiar to most physicists, quantum perturbation theory.[16] These efforts sometimes may give conducive, intuitive analytic formulas of diffraction efficiencies that can be used for the evaluation of trend or further analytical studies. In this regard, our approach may have a unique value as well.

As we mentioned earlier, the unit cell could be an arbitrary parallelogram with its base parallel to the grating surface. If the grating profile has its intrinsic geometric boundaries following the slanting side of a parallelogram, then a nonrectangular unit cell may be beneficial. Note that our method can handle this type of problem as well, but the right-hand side of Eqs. (10) or (12) must be modified with b_{1y} explicitly present as discussed earlier.

It is possible to choose an alternative structure for the virtual photonic crystal as shown in Fig. 4(b). Correspondingly, one needs to solve the boundary condition at

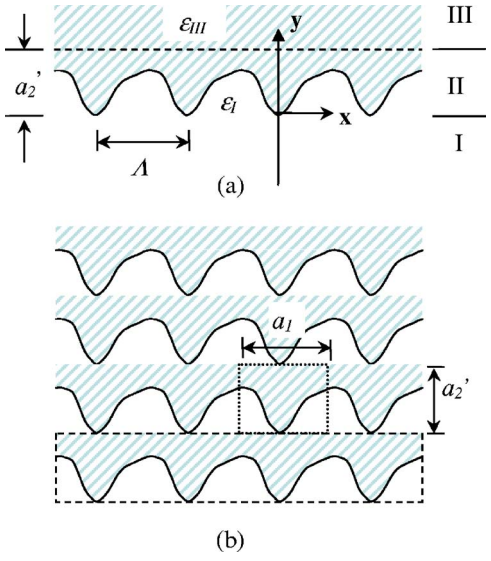

Fig. 4. (Color online) Alternative choice of the virtual photonic crystal. (a) Region II has to be redefined (now between $y=0$ and $y=a_2'$). And the backside boundary is now located at $y=a_2'$. (b) The corresponding 2D photonic crystal. A unit cell is indicated by dotted lines. The layer actually present in the grating problem is enclosed by dashed lines.

Table 1. Comparison of Diffraction Efficiencies with Those in Ref. 2

Diffraction Order[a]	λ/Λ	Ref. 2	Present Work
$DE_{3,0}$	0.750	0.15377	0.15624
$DE_{3,1}$	0.750	0.57732	0.57615
$DE_{3,2}$	0.750	0.20013	0.20027
$DE_{3,0}$	0.941	0.30290	0.30319
$DE_{3,1}$	0.941	0.63689	0.63727
$DE_{3,2}$	0.941	0.05058	0.05137
$DE_{3,0}$	1.030	0.34202	0.34361
$DE_{3,1}$	1.030	0.62361	0.62442
$DE_{3,2}$	1.030	0.02398	0.02256
$DE_{3,0}$	1.177	0.39857	0.39920
$DE_{3,1}$	1.177	0.59051	0.59082
$DE_{3,2}$	1.777	0.00000	0.00000
$DE_{3,0}$	1.471	0.49355	0.49489
$DE_{3,1}$	1.471	0.49134	0.48980
$DE_{3,2}$	1.471	0.00000	0.00000

[a] $DE_{3,i}$ is the ith-order diffraction efficiency in medium III.

$y=a_2'$, rather than at $y=d$, as shown in Fig. 4(a). Any proper choice of virtual photonic crystal will not affect the calculated values of diffraction efficiency just as any proper choice of contour does not affect the value of a complex contour integral. However, any choice with $a_2'>d$ would generally require extra Fourier components to represent the enlarged unit cell. This unnecessarily increases the computational workload and complicates the calculation, and therefore it is not used.

In Table 1 we compare our numerical results with those of Ref. 2 for a sinusoidal surface-relief grating with $\varepsilon_I=1.0$, $\varepsilon_{III}=2.3104$, and $d/\Lambda=1.1765$. The incident angle is 36°. Our results are in excellent agreement with the results listed in Table 3 of the widely cited work by Moharam and Gaylord.[2] All results in the present work are obtained with L, M in the range of 12–20.

5. CONCLUSION

In summary, a rigorous theory of grating diffraction is developed based on the concept of virtual photonic crystals. Our method separates the calculation of the Fourier coefficients of a grating from the diffraction efficiency calculation, and analytical forms of Fourier coefficients can be used for many common surface-relief profiles. In two simple steps, diffraction efficiencies can be calculated from the 2D Fourier series of the dielectric function without slicing the grating profile into thin layers. Directions for further study have been discussed.

ACKNOWLEDGMENTS

The authors are indebted to Lifeng Li of Tsinghua University, Beijing, China, for extensive helpful discussions. We thank J. Chen for reading the paper and providing comments. This work is supported in part by the U.S. Air Force Research Laboratory. The authors also acknowledge partial support from the U.S. Air Force Office of Scientific Research.

Author W. Jiang can be reached by e-mail at jiang@ece.utexas.edu.

REFERENCES

1. H. Kogelnik, "Coupled wave theory for thick hologram gratings," Bell Syst. Tech. J. **48**, 2909–2947 (1969).
2. M. G. Moharam and T. K. Gaylord, "Diffraction analysis of dielectric surface-relief gratings," J. Opt. Soc. Am. **72**, 1385–1392 (1982).
3. L. Li, "Multilayer modal method for diffraction gratings of arbitrary profile, depth, and permittivity," J. Opt. Soc. Am. A **10**, 2581–2591 (1993).
4. N. Chateau and J. P. Hugonin, "Algorithm for the rigorous coupled-wave analysis of grating diffraction," J. Opt. Soc. Am. A **11**, 1321–1331 (1994).
5. M. G. Moharam, D. A. Pommet, E. B. Grann, and T. K. Gaylord, "Stable implementation of the rigorous coupled-wave analysis for surface-relief gratings: enhanced transmittance matrix approach," J. Opt. Soc. Am. A **12**, 1077–1086 (1995).
6. L. Li, "Formulation and comparison of two recursive matrix algorithms for modeling layered diffraction gratings," J. Opt. Soc. Am. A **13**, 1024–1035 (1996).
7. R. T. Chen, H. Lu, D. Robinson, and T. Jannson, "Highly multiplexed graded-index polymer waveguide hologram for near-infrared eight-channel wavelength division demultiplexing," Appl. Phys. Lett. **59**, 1144–1146 (1991).
8. M. R. Wang, G. J. Sonek, R. T. Chen, and T. Jannson, "Large fanout optical interconnects using thick holographic gratings and substrate wave propagation," Appl. Opt. **31**, 236–249 (1992).
9. L. Gu, X. Chen, Z. Shi, B. Howley, J. Liu, and R. T. Chen, "Bandwidth-enhanced volume grating for dense wavelength-division multiplexer using a phase-compensation scheme," Appl. Phys. Lett. **86**, 181103 (2005).
10. L. Gu, X. Chen, W. Jiang, and R. T. Chen, "A solution to the fringing-field effect in liquid crystal based high-resolution switchable gratings," Appl. Phys. Lett. **87**, 201106 (2005).
11. H. Kosaka, T. Kawashima, A. Tomita, M. Notomi, T. Tamamura, T. Sato, and S. Kawakami, "Superprism phenomena in photonic crystals," Phys. Rev. B **58**, R10096 (1998).
12. W. Jiang, R. T. Chen, and X. Lu, "Theory of light refraction at the surface of a photonic crystal," Phys. Rev. B **71**, 245115 (2005).
13. P. Lancaster, *Lambda-Matrices and Vibrating Systems* (Pergamon, 1966).
14. W. Jiang, "Wavelength-selective micro- and nano-photonic devices for wavelength division multiplexing networks," Ph.D. dissertation (University of Texas at Austin, 2005).
15. J. H. Wilkinson, *The Algebraic Eigenvalue Problem* (Clarendon, 1965).
16. L. I. Schiff, *Quantum Mechanics*, 3rd ed. (McGraw-Hill, 1968).